*American Journal of Materials Science and Engineering, 2018, Vol. 6, No. 2, 37-42*
Available online at http://pubs.sciepub.com/ajmse/6/2/3

DOI:10.12691/ajmse-6-2-3

# Mesostructured Hybrid based-Perovskite Solar Cell Optical and Electrical Modeling: Influence of the Incident Light Wavelength

**Allé Dioum[1,2], Abdoulaye Ndiaye Dione[1,2,*], El Hadji Oumar Gueye[1,2], Sossé Ndiaye[1], Aboubaker Chedikh Beye[1]**

[1]Physical Solid and Material Sciences Group, Department of Physics (GPSSM), University of Cheikh Anta Diop, Dakar, Senegal
[2]Material and Composite Systems for Energy Applications (MASCA), Department of Physics, University of Cheikh Anta Diop, Dakar, Senegal
*Corresponding author: ndigualdione@gmail.com

*Received October 10, 2018; Revised November 12, 2018; Accepted November 21, 2018*

**Abstract** Analytical model is developed to give insight into the influence of the incident wavelength of the incoming light illumination on optical and electrical properties mesostructured hybrid perovskite-based solar cell for different photoactive layer thickness. Bruggeman theory and T-matrix are used to compute the analytical expressions of optical parameters such as absorption coefficient and generation rate. Then, the short-circuit current density is deduced from the continuity equation. The absorption coefficient of the photoactive layer decreases with high incident wavelength of the incoming light of the visible spectrum (400-800 nm) while the absorbance and generation rate grow up with the phototactive layer thickness. The current density increases with illuminated wavelength ranging 400-520 nm while it decreases with higher active medium ($TiO_2$ +Perovskite) layer thickness ranging from 500 nm to 1.7 µm. Beyond to 520 nm of the wavelength of the incoming light, the current density decreases to vanish at 800 nm. As finding in the literature, it can be noticed high absorption, charge carriers generation and current density for low wavelength in the visible spectrum which correspond to high energies.

***Keywords:*** *Modelling, Hybrid solar cell, perovskite, Mesostructure, Bruggeman theory, T-matrix*

**Cite This Article:** Allé Dioum, Abdoulaye Ndiaye Dione, El Hadji Oumar Gueye, and Sossé Ndiaye, "Mesostructured Hybrid based-Perovskite Solar Cell Optical and Electrical Modeling: Influence of the Incident Light Wavelength." *American Journal of Materials Science and Engineering*, vol. 6, no. 2 (2018): 37-42. doi: 10.12691/ajmse-6-2-3.

## 1. Introduction

Recently, the investigation of hybrid perovskite-based solar cells attract the attention of scientific community around the world because of their important and remarkable luminous characteristics [1]. The first paper on perovskite solar cells was published in 2009 by Akihiro Kojima and al., with low conversion efficiencies of 3.13% and 3.81% [2]. Several investigations have been developed to improve their efficiency [3-19]. Due to their rapid evolution, perovskite are very competitive compared to the third generation of photovoltaic devices (organic solar cells) and conventional (silicon) technologies which have been studied in the last decades. A record conversion efficiency of about 22.1% has been certified in 2016 [21]. There is a series of organic-inorganic perovskite materials ($CH_3NH_3AX_3$) where M is a metal (M = Pb, Sn) and X is a halogen (X = I, Br, Cl). Meanwhile, perovskite materials $CH_3NH_3PbI_{3-x}cl_x$ (x=0;1 ;2 ;3) are much more widely used, with very good efficiencies [22-28]. These perovskite-based organic-inorganic hybrid cells are derived from the so-called third-generation dye-like cells commonly referred to as "Grätzel solar cell conception".

To date two different architectures exist: mesostructure and plane structures.

Mesostructure consisting of titanium dioxide ($TiO_2$) and perovskite ($CH_3NH_3PbI_3$) layer sandwiched between an anode transparent electrode and a metal cathode electrode as depicting in Figure 1. Many experimental investigations have been devoted to the mesostructure perovskite solar cells in the last years [2-7]. However, theoretical models to predict and optimize parameters affected the devices efficiency are almost unexisted.

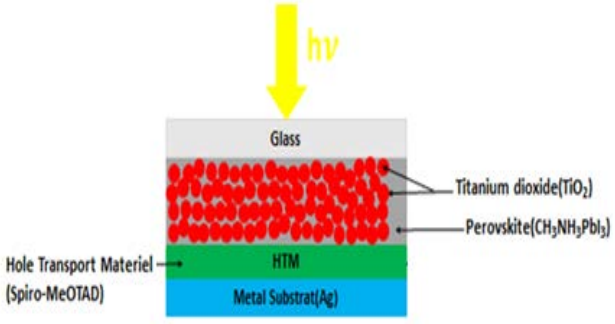


**Figure 1.** Schematic model of mesostructured hybrid based-perovskite solar cell

Our present analytical and numerical model is developed to give insight into the dependence effects of wavelength of the incoming light and the medium ($TiO_2$+Perovskite) layer thickness on the absorption, the charge carrier generation and the current density.

## 2. Computational Model

Computational results consisting of determining in one hand optical parameters such as the absorption and the charge carriers generated within the photoactive layer ($TiO_2$+ $CH_3NH_3PbI_3$) and in other hand the electrical parameters as short-circuit current are presented in this section.

Some assumptions are considered to determine the absorption of the photoactive layer which consisting of a blending of nanoparticles of $TiO_2$ and methylammonium lead iodide perovskite. In this part, only the photoactive layer is considered and represented as below in Figure 2.

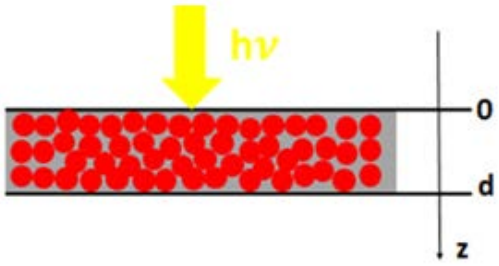


**Figure 2.** Schematic model of the photoactive layer consisting of $TiO_2$ and $CH_3NH_3PbI_3$ perovskite

One dimensional Cartesian system is associated to the active layer. The origin is taken at the anode/photoactive interface, z the depth and d the thickness.

### 2.1. Optical Computation

This part is devoted to the determination of the optical parameters of the composite photoactive layer ($TiO_2$+$CH_3NH_3PbI_3$) such as the absorption coefficient, the absorbance and the generation rate. These parameters depend on the refractive index of the composite material. However, the individual elements refractive indexes of titanium dioxide ($TiO_2$) and $CH_3NH_3PbI_3$ for the visible spectrum wavelength ranging from 400 nm to 800 nm are obtained from the literature [29].

Consequently, the refractive index of the photoactive layer is calculated by using Bruggeman theory (effective medium theory) which takes in spherical shape the nanoparticles [30-34]. This theory leads to a second-degree equation given by relation (1):

$$2\varepsilon_m^2 + \left[(3p-2)\varepsilon_a + (1-3p)\varepsilon_b\right]\varepsilon_m - \varepsilon_a\varepsilon_b = 0 \quad (1)$$

Where $\varepsilon_m$ is the average dielectric constant of the composite medium, $\varepsilon_a$ and $\varepsilon_b$ are the dielectric permittivity of $TiO_2$ and perovskite respectively, $p$ the porosity of $TiO_2$ [35].

The resolution of equation(1) leads to the average dielectric constant of the composite medium which allows to deduce the refractive index complex ( $N$ ) given by the equation (2):

$$\varepsilon_m = N^2 \quad (2)$$

with

$$N = n - jk \quad (3)$$

$n$ and $k$ being respectively the refractive index and extinction coefficient of the composite medium.

Finally, the analytical expression of the absorption coefficient of the photoactive layer is given by equation (4):

$$\alpha(\lambda) = \frac{4\pi k}{\lambda}. \quad (4)$$

To determine the absorbance of the solar cell, the previous consider a photoactive layer is deposited on flat glass. The stacking thin layers is as shown in Figure 3.

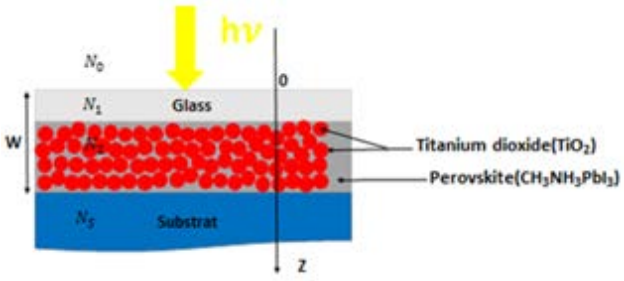


**Figure 3.** Schematic model of a stacking thin layers

The stacking thin films method so-called T-matrix is used to determine the electrical field component which depend on the parameters of the matrix given by equation (5) as below [30]:

$$\begin{pmatrix} E(0) \\ H(0) \end{pmatrix} = \prod_{i=1}^{m} M_i \begin{pmatrix} E(w) \\ H(w) \end{pmatrix} \quad (5)$$

$E$ and $H$ are the amplitudes of the fields $\vec{E}$ and $\vec{H}$, at the input ( $z = 0$ ) and the output ( $z = w$ ) of the stack. $w$ being the thickness of the stack. $M_i$ is the equivalent matrix of the $i$ layer given by equation(6):

$$M_i = \begin{pmatrix} \cos\varphi_i & \frac{j}{Y_i}\sin\varphi_i \\ jY_i\sin\varphi_i & \cos\varphi_i \end{pmatrix} \quad (6)$$

$Y_i$ and $\varphi_i$ are the wave admittance in the layer $i$ and the phase shift undergone by the wave when it passes through the layer $i$ respectively. By simplifying, equation (5) leads to:

$$\begin{pmatrix} B \\ C \end{pmatrix} = \prod_{i=1}^{m} M_i \begin{pmatrix} 1 \\ Y_S \end{pmatrix} \quad (7)$$

$Y_S$ being the admittance wave in the substrate. Parameters $B$ and $C$ are defined by the following relations:

$$B = \frac{E(0)}{E(w)} \quad (8)$$

$$C = \frac{H(0)}{E(w)}. \quad (9)$$

The optical parameters such as the reflectance ( $R$ ), transmittance ( $T$ ) and absorbance ( $A$ ) of a stack of thin layers, are given below and depend on B and C the parameters matrix [36].

$$R = \left(\frac{Y_0 B - C}{Y_0 B + C}\right)\left(\frac{Y_0 B - C}{Y_0 B + C}\right)^* \tag{10}$$

$$T = \frac{4Y_0 \,\mathrm{Re}(Y_S)}{(Y_0 B + C)(Y_0 B + C)^*} \tag{11}$$

$$A = 1 - (R + T) \tag{12}$$

$Y_0$ is the admittance of the wave in a vacuum.

Using calculations based on electromagnetism and considering the static energy conservation equation [36] defined by equation (13), one can easily obtain the electron generation rate in term of the stacking layers depth $z$ for the wavelength of the monochromatic incident light as in -equation(14) considering equation (13).

$$Q + div\vec{P} = 0 \tag{13}$$

with $Q$, total energy density per unit of time and $\vec{P}$ , Poynting Vector.

$$G_e(z,\lambda) = \eta_{inj} G_a(z,\lambda) \tag{14}$$

$\eta_{inj}$ being the photons injection rate.

The photon absorption rate is given by equation (15):

$$G_a(z,\lambda) = \frac{Q(z,\lambda)}{\frac{hc}{\lambda}} \tag{15}$$

where,

$$Q(z,\lambda) = \frac{1}{2}\alpha(\lambda).N.Y.|E|^2 \tag{16}$$

$h$ and c are Planck constant and the velocity of light in vacuum respectively. $E$ and $Y$ being the electric field amplitude and the wave admittance in the photoactive layer respectively.

## 2.2. Electrical Computation

The analytical expression of the short-circuit current density is computed in this section. The perovskite material is the main responsible of incoming light absorption within the photoactive layer. Actually, all the mechanism such as the charge carriers transport, recombination are carried out within the photoactive layer identically in dye sensitized solar cells (DSSCs). It can be noticed that electrons conduction predominance in charge transport of conduction through mesoporous titanium dioxide ($TiO_2$) [37].

It has also been suggested that the high dielectric constant of perovskite material allows photo-generated excitons to dissociate immediately into free carriers (electrons and holes) [5,38]. Under illumination, electrons photogenerated diffuse through the photoactive layer to be collected at the anode electrode.

Therefore, it is important to develop electrical model to solve the steady-state equation of electron density across the photoactive layer [39] defined as below:

$$\frac{\partial^2 \rho(z)}{\partial z^2} - \frac{\rho(z)}{L^2} + \frac{G_e(z)}{D} = 0 \tag{17}$$

where, $\rho(z)$ is electrons density in term of the depth $z$ . $D$ and $L$ are the diffusion coefficient and length respectively. $G_e(z)$ represents the electron generation rate in various wavelength of the light.

In order to resolve equation (17), charge carriers recombinations within the photoactive region are negligible because their diffusion length is very important compared to the layer thickness in the perovskite material [40,41].

To ensure the unicity of the solution of equation (17), the following boundary conditions at the anode/active layer ( $z = 0$ ) and active layer/cathode ( $z = d$ ) interfaces respectively:

$$\frac{\partial \rho(z)}{\partial z}\Big|_{z=0} = \frac{S_1}{D}\rho(0) \tag{18}$$

$$\frac{\partial \rho(z)}{\partial z}\Big|_{z=d} = \frac{-S_2}{D}\rho(d). \tag{19}$$

where $S_1$ and $S_2$ denote the recombination rates of the electrons at the interfaces ( $z = 0$ ) and ( $z = d$ ) respectively.

Finally, the short-circuit current density is deduced from the electrons density photogenerated within the photoactive layer and shown in equation (20):

$$J_{cc} = qD\frac{\partial \rho(z)}{\partial z}\Big|_{z=0}. \tag{20}$$

where $q$ is the electron charge.

# 3. Results and Discussions

The analytical expressions of the optical and electrical parameters are depicted by establishing a numeric based-code implemented by the commercial software Matlab. The numerical results are presented in this section.

The composite layer ($TiO_2$+ $CH_3NH_3PbI_3$) absorption coefficient, the absorbance, charge carrier generation rate and the short-circuit current density as a function of the incoming light wavelength for various thickness are presented and discussed.

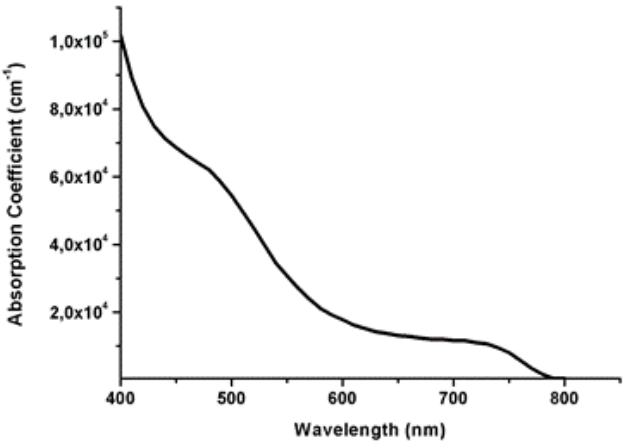


**Figure 4.** Absorption coefficient of the composite photoactive layer as a function of the incident light wavelength

The Figure 4 shows the absorption coefficient of the photoactive layer as a function of the incident light wavelength of the spectrum of the visible.

The absorption coefficient decreases the high incoming light wavelength while it increases with high energies as summarize in N.G. Park studies [20].

It can be predicted form this result, the variation of others optical parameters such as $\lambda$, $\alpha$ and $A$ depending on the parameters of the matrix.

In Figure 5 is depicted the absorbance versus the incident light wavelength for different thickness of the absorber layer.

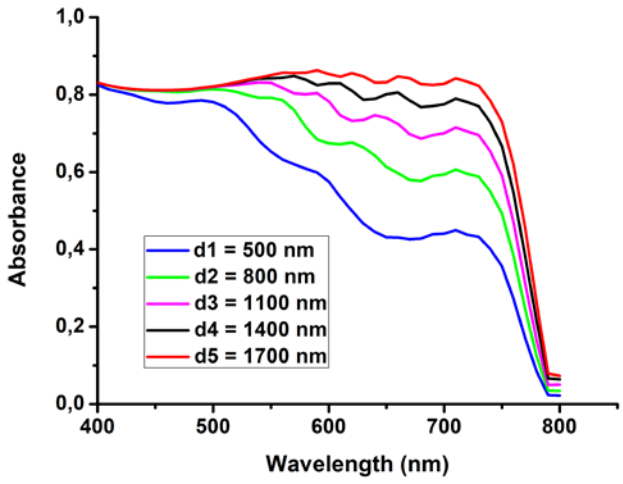


**Figure 5.** Theoretical absorbance of the solar cell as a function of the incident wavelength in the visible range for different thicknesses of the photoactive layer

The absorbance shows various pics in different magnitudes which decreases very quickly with high incident light wavelength of the spectrum of the visible to vanish at 800 nm while it increases for high thickness ranging from 500 nm to 1.7µm. This decrease of the absorbance can be noticed with low thickness around 500 nm for the wavelength ranging from 500 nm to 725 nm.

These results are in good agree with G. Sfyrie & al. for any fixed thickness [42]. The results give insight into the dependence effects of the both the incident light wavelength in the spectrum of the visible and the medium ($TiO_2$+perovskite) region thickness on the absorbance of the absorber material. It can be predicted that the blend of $TiO_2$ and $CH_3NH_3PbI_3$ perovskite has a large band of absorption in the spectrum of the visible ranging from 500nm to 775 nm and the limited value of thickness to deposit on substrate in order to obtain high magnitude of absorbance for photovoltaic conversion and efficiency.

Charge carriers are photogenerated within the medium region subsequent to the absorption of the incoming light excitation. The absorption coefficient and the absorbance are used to investigate the charge carriers generation rate.

Figure 6 shows the charge carriers generation rate versus the incident light wavelength for different thickness of the photoactive layer (TiO2+ $CH_3NH_3PbI_3$).

The charge carrier generation rate decreases with the incident light wavelength by exhibiting two pics at 500 nm and 725 nm. The former presents high magnitude ($3.4x10^{20}cm^{-3}$) compared to the latter ($7.5x10^{19}cm^{-3}$). It vanishes with highest wavelengths at 775 nm. Compared to the absorbance, the charge carriers generation increases very slowly with high thickness ranging from 500 nm to 1.7 µm.

Subsequently to the charge carriers generation within the photoactive layer consisting of blending of $TiO_2$ and $CH_3NH_3PbI_3$ absorber material, electrons diffuse towards the electrodes to be collected as current. Consequently, one can be said that the short-circuit current of the cell is related to the active region absorption. The short-circuit current density versus the incident wavelength for different thickness is depicted in Figure 7.

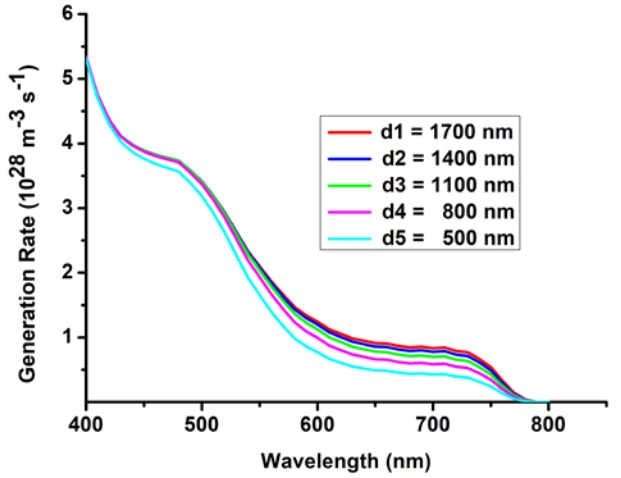


**Figure 6.** Generation rate of electrons as a function of the incident wavelength in the visible range for different thicknesses of the photoactive layer

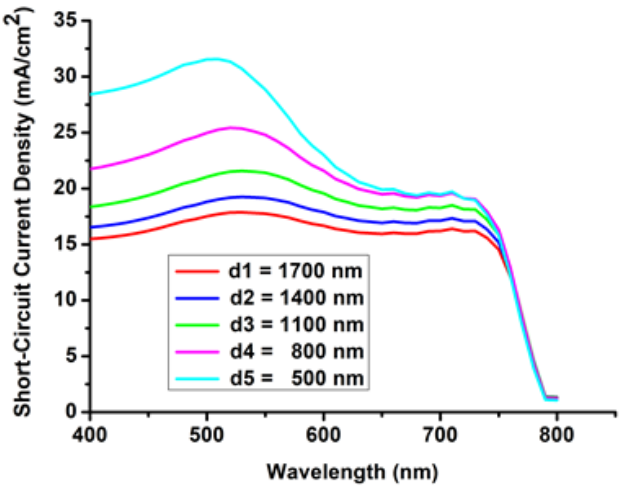


**Figure 7.** Short-circuit current density as a function of the incident wavelength in the visible range, for different thicknesses of the photoactive layer

Figure 7 depicts the short-circuit current density as a function of the wavelength for different thicknesses of photoactive composite layer.

The current density increases with illuminated wavelength ranging 400-520 nm while it decreases with higher active layer thickness ranging from 500-1700 nm. Beyond to 520 nm of the wavelength of the incoming light, the current density decreases slowly then quickly to vanish at 800nm. In term of the active layer thickness, the current density grows weakly due to the limited charge carriers diffusion length ranging 1200-1500 nm [37]. Basically, charge

collection is as well as higher the active layer thickness being less than the charge carriers diffusion length for the illumination wavelength ranging 400-775 nm while no effect could not be affect beyond this region. Consequently, the short-circuit current density of about 24 $mA.cm^{-2}$ is recorded for 670 nm thickness under 400 nm illumination. These results are in good agreement with G.Sfyrie and al. [42].

# 4. Conclusion

From our model we have been able to investigate the influence of the wavelength of the incident light for different thicknesses of the composite photoactive layer, on the optical and electrical properties of a hybrid solar cell based on perovskite material $CH_3NH_3PbI_3$ mesostructured. This model allowed us to know the efficiency of the solar cell considered on the absorption of light, the generation of electrons and currents in the visible wavelength range. We have also found that in the visible domain, the absorption of light and the generation of charge carriers and currents are much greater for the low wavelengths corresponding to the large energies. However, it would be interesting to investigation the internal and external quantum yields of the whole cell for better optimization.

# References


[1] De Wolf, S., Holovsky, J., Moon, S. J., Lö per, P., Niesen, B., Ledinsky, M., Haug, F.J., Yum, J.H., and Ballif, C., "Organometallic Halide Perovskites: Sharp Optical Absorption Edge and Its Relation to Photovoltaic Performance", *Journal of Physical Chemistry Letters*, 5(6). 1035-1039. March.2014.

[2] Kojima, A., Teshima, K., Shirai, Y., and Miyasaka, T., "Organometal Halide Perovskites as Visible-Light Sensitizers for Photovoltaic Cells,", *Journal of the American Chemical Society*, 131(17). 6050–6051. April. 2009.

[3] Im, J. H., Lee, C. R., Lee, J. W., Park, S. W., and Park, N. G., "6.5% efficient perovskite quantum-dot-sensitized solar cell", Nanoscale, 3(10). 4088-4093. September. 2011.

[4] Kim, H. S., Lee, C. R., Im, J. H., Lee, K. B., Moehl, T., Marchioro, A., Moon, S. J., Baker, R. H., Moser, J.E., Grätzel, M., and Park, N.G., "Lead iodide perovskite sensitized all-solid-state submicron thin film mesoscopic solar cell with efficiency exceeding 9%", *Scientific reports*, 2. August. 2012.

[5] Lee, M. M., Teuscher, J., Miyasaka, T., and Murakami, T., "Efficient hybrid solar cells based on meso-superstructured organometal halide perovskites", *Science*, *338*(6107). 643-647. November. 2012.

[6] Etgar, L., Gao, P., Xue, Z., Peng, Q., Chandiran, A. K., Liu, B., Nazeeruddin, M. K., and Grätzel, M., "Mesoscopic $CH_3NH_3PbI_3$ /$TiO_2$ heterojunction solar cells", *Journal of the American Chemical Society*, *134*(42). 17396-17399. October. 2012.

[7] Im, J. H., Chung, J., Kim, S. J., and Park, N. G., "Synthesis, structure, and photovoltaic property of a nanocrystalline 2H perovskite-type novel sensitizer ($CH_3NH_3PbI_3$)", *Nanoscale research letters*, *7*(1). 353. June. 2012.

[8] Liu, D., and Kelly, T. L., "Perovskite solar cells with a planar heterojunction structure prepared using room-temperature solution processing techniques", *NATURE PHOTONICS*, *8*(2). 133-138. December. 2013.

[9] Bi, D., Yang, L., Boschloo, G., Hagfeldt, A., and Johansson, E. M., "Effect of Different Hole Transport Materials on Recombination in $CH_3NH_3PbI_3$ Perovskite Sensitized Mesoscopic Solar Cells", *Journal of Physical Chemistry Letters*, 4 (9). 1532-1536. April. 2013.

[10] Snaith, H. J., "Perovskites: the emergence of a new era for low-cost, high-efficiency solar cells", *The Journal of Physical Chemistry Letters*, *4*(21). 3623-3630. 2013.

[11] Boix, P. P., Nonomura, K., Mathews, N., and Mhaisalkar, S. G., "Current progress and future perspectives for organic/inorganic perovskite solar cells", *Materials today*, *17*(1). 16-23. January/February. 2014.

[12] Zhang, J., Barboux, P., and Pauporté, T., "Electrochemical Design of Nanostructured ZnO Charge Carrier Layers for Efficient Solid-State Perovskite-Sensitized Solar Cells", *Advanced Energy Materials*, *4*(18). September. 2014.

[13] Nagarjuna, P., Narayanaswamy, K., Swetha, T., Rao, G. H., Singh, S. P., and Sharma, G. D., "$CH_3NH_3PbI_3$ Perovskite Sensitized Solar Cells Using a D-A Copolymer as Hole Transport Material", *Electrochimica Acta*, 151(1). 21-26. January. 2015.

[14] Wei, H., Xiao, J., Yang, Y., Lv, S., Shi, J., Xu, X., Dong, J., Luo, Y., Li, D., and Meng, Q., "Free-standing flexible carbon electrode for highly efficient hole-conductor-free perovskite solar cells", *Carbon*, *93*. 861-868. November. 2015.

[15] Wang, K., Liu, C., Du, P., Chen, L., Zhu, J., Karim, A., and Gong, X., "Efficiencies of perovskite hybrid solar cells influenced by film thickness and morphology of $CH_3NH_3PbI_{3-x}cl_x$ layer", *Organic Electronics*, *21*. 19-26. June. 2015.

[16] Tao, H., Ke, W., Wang, J., Liu, Q., Wan, J., Yang, G., and Fang, G., "Perovskite solar cell based on net work nanoporous layer consisted of $TiO_2$ nanowires and its interface optimization", *Journal of Power Sources*, 290. 144-152. September. 2015.

[17] Brenner, T. M., Egger, D. A., Kronik, L., Hodes, G., and Cahen, D., "Hybrid organic–inorganic perovskites:low-cost semiconductors with intriguing charge-transport properties", *Nature Reviews Materials*, *1*. 15007. January. 2016.

[18] Mehmood, U., Al-Ahmed, A., Afzaal, M., Al-Sulaiman, F. A., and Daud, M., "Recent progress and remaining challenges in organometallic halides based perovskite solar cells", *Renewable and Sustainable Energy Reviews*, *78*. 1-14. October. 2017.

[19] Chen, Q., Chen, L., Ye, F., Zhao, T., Tang, F., Rajagopal, A., Jiang, Z., Jiang, S., Jen, A. K. Y., Xie, Y., Cai, J., and Chen, L., "Ag-Incorporated Organic-Inorganic Perovskite Films and Planar Heterojunction Solar Cells", *Nano Letters*, 17(5). 3231-3237. March. 2017.

[20] Park, N. G., "Perovskite solar cells: an emerging photovoltaic", *Materials Today*, 18(2). 65-72. March. 2015.

[21] Da, P., and Zheng, G., "Tailoring interface of lead-halide perovskite solar cells", *Nano Research*, 10(5). 1471-1497. May. 2017.

[22] Yang, W. S., Noh, J. H., Jeon, N. J., Kim, Y. C., Ryu, S., Seo, J., and Seok, S. I., "High-performance photovoltaic perovskite layers fabricated through intramolecular exchange", *Science*, 348(6240). 1234-1237. June. 2015.

[23] Ko, H. S., Lee, J. W., and Park, N. G., "15.76% Efficiency Perovskite Solar Cell Prepared under High Relative Humidity: Importance of $PbI_2$ Morphology in Two-Step Deposition of $CH_3NH_3PbI_3$", *Journal of Materials Chemistry A*, *3*(16). 8808-8815. March. 2015.

[24] Huang, F., Dkhissi, Y., Huang, W., Xiao, M., Benesperi, I., Rubanov, S., Zhu, Y., Lin, X., Jiang, L., Zhou, Y., Gray-Weale, A., Etheridge, J., McNeill, C. R., Caruso, R. A., Bach, U., Spiccia, L., and Cheng, Y. B., "Gas-assisted preparation of lead iodide perovskite films consisting of a monolayer of single crystalline grains for High efficiency planar solar cells", *Nano Energy*, 10. 10-18. November. 2014.

[25] Yang, Z., Cai, B., Zhou, B., Yao, T. T., Yu, W., Liu, S.Z., Zhang, W. H., and Li, C., "An up-scalable approach to $CH_3NH_3PbI_3$ compact Films for High-performance perovskite solar cells", *Nano Energy*, 15(0). 670. December. 2015.

[26] Zhou, H., Chen, Q., Li, G., Luo, S., Song, T. B., Duan, H. S., Hong, Z., You, J., Liu, Y., and Yang, Y. "Interface engineering of highly efficient perovskite solar cells", *Science*, *345*(6196). 542-546. August. 2014.

[27] Zhu, L., Shi, J., Lv, S., Yang, Y., Xu, X., Xu, Y., Xiao, J., Wu, H., Luo, Y., Li, D., and Meng, Q., "Temperature-assisted controlling morphology and charge transport property for highly efficient perovskite solar cells", *Nano Energy*, 15. 540-548. July.2015.

[28] Burschka, J., Pellet, N., Moon, S. J., Humphry-Baker, R., Gao, P., Nazeeruddin, M. K., and Grätzel, M., "Sequential deposition as a route to high-performance perovskite-sensitized solar cells", *Nature*, 499. 316-319. July. 2013.

[29] Palik, E. D and Ghosh, G. *Handbook of Optical Constants of Solids, Academic Press, Orlando*, 1985, 577-580.

[30] S. Berthier and J. Lafait. "Modelisation des proprietes optiques des milieux inhomogenes a structure complexe", *Journal de Physique Colloques*, 42 (1), Jan 1981.

[31] A.M.Jayannavar and N.Kumar, "Generalization of Bruggeman's unsymmetrical effective medium theory to a three-component composite", *Physical Review*, 44(21), December 1991.

[32] M.Louge and M.Opie, "Measurements of the effective dielectric permittivity of suspensions", *Powder Technology*, 62(1), July 1990.

[33] P. Mallet, "Diffusion électromagnétique par des matériaux hétérogènes rugueux: homogénéisation et étude du couplage", Thèse de doctorat. Aix-Marseille 3, France, 2006.

[34] S. Orlowska, "Conception et prédiction des caractéristiques diélectriques des matériaux composites à deux et trois phases par la modélisation et la validation expérimentale", Thèse de doctorat, Ecole Centrale De Lyon, France, 2003.

[35] Gueye, E.H.O., Tall, P.D., Ndao, C.B., Dioum, A., Dione, A.N and Beye, A.C, "An Optical and Electrical Modeling of Dye Sensitized Solar Cell: Influence of the Thickness of the Photoactive Layer", *American Journal of Modeling and Optimization*, 4(1). 13-18. 2016.

[36] D. Allé "Etude en 3D de cellules photoactives organiques bicouches composées de phthalocyanine de cuivre (CuPc) et de fullerene ($C_{60}$): Influence de la dissociation des excitons aux interfaces actives", thèse de doctorat de troisième cycle, Université Cheikh Anta Diop de Dakar, Sénégal, 2010.

[37] Zhao, Y., Nardes, A. M., and Zhu, K., "Solid-State Mesostructured Perovskite $CH_3NH_3PbI_3$ Solar Cells: Charge Transport, Recombination, and Diffusion Length", *Journal of Physical Chemistry Letters*, 5(3). 490-494. January. 2014.

[38] D'Innocenzo, V., Grancini, G., Alcocer, M. J. P., Kandada, A. R. S., Stranks, S. D., Lee, M. M., Lanzani, G., Snaith, H. J., and Petrozza, A., "Excitons versus free charges in organo-lead tri-halide perovskites", *Nature communications*, 5. 3586. April. 2014.

[39] Sun, X., Asadpour, R., Nie, W., Mohite, A. D., and Alam, M. A., "A physics-based analytical model for perovskite solar cells", *IEEE Journal of Photovoltaics*, *5*(5). 1389-1394. September 2015.

[40] Dong, Q., Fang, Y., Shao, Y., Mulligan, P., Qiu, J., Cao, L., and Huang, J., " Electron-hole diffusion lengths >175 m in solution grown $CH_3NH_3PbI_3$ single crystals", *Science*, 347(6225). 967-970. February. 2015.

[41] Gonzalez-Pedro, V., Juarez-Perez, E. J., Arsyad, W.-S., Barea, E. M., Fabregat-Santiago, F., Mora-Sero, I and Bisquert, J, "General Working Principles of $CH_3NH_3PbI_3$ Perovskite Solar Cells", Nano Letters, 14(2). 888-893. January. 2014.

[42] Sfyri, G., Kumar, C. V., Raptis, D., Dracopoulos, V., and Lianos, P., "Study of perovskite solar cells synthesized under ambient conditions and of the performance of small cell modules". *Solar Energy Materials and Solar Cells*, *134*, 60-63. March. 2015.

[43] Dione, A. N., Ndiaye, S., El Hadji Oumar Gueye, A. D., Diouf, A. A., Abderaman, M. B., Ngom, B. D., and Beye, A. C., "Optical and Electrical Modeling of a hybrid Solar Cell based on a Mesostructured Perovskite CH3NH3PbI3: Influence of the Depth and Thickness of the Photoactive Layer", *American Journal of Nanomaterials*, *5*(2). 68-71. December. 2017.